73rd International Astronautical Congress (IAC), Paris, France, 18-22 September 2022.

IAC-22,D2,6,7,x69473

Objectives and Achievements of the Hypersonic Flight Experiment STORT

A. Gülhan[a]*, D. Hargarten[b], M. Zurkaulen[b], F. Klingenberg[a], F. Siebe[a], G. die Martino[c], T. Reimer[c]

[a] *Supersonic and Hypersonic Technologies Department, Institute of Aerodynamics and Flow Technology, German Aerospace Center (DLR), Cologne, Germany*
[b] *Mobile Rocket Base (MORABA) Department, Institute of Space Operations and Astronaut Training, German Aerospace Center (DLR), Oberpfaffenhofen, Germany*
[c] *System Integration Department, Institute of Structures and Design, German Aerospace Center (DLR, Stuttgart, Germany*
* Corresponding Author (Ali.Guelhan@dlr.de)

Abstract

The three-stage rocket configuration of the hypersonic experiment STORT with several scientific payloads concerning hypersonic technologies was launched from the Andøya Space launch site in northern Norway on 26th June 2026 successfully. The third stage performed a suppressed trajectory to increase integral heat load on the structures of payloads. The duration of a flight phase above Mach 8 at altitudes between 30 km and 38 km was more than 60 seconds. The nose and forebody section of the payload is made of the CMC structures. Three canards with a CMC thermal protection were equipped with thermal management experiments to verify the thermal efficiency of these methods. All engineering science experiments like aerothermal heating of the nose and forebody, CMC material response at temperatures above 2200 K, hypersonic thermal management, shock wave boundary layer interaction, CFRP module with cork coating for high temperature applications, high temperature fin leading edge and radiometer sensors provided unique flight data. A reduced in-flight 3 DoF trajectory simulation running on the flight computer determined the ignition time of the third stage which allowed improved experiment conditions in terms of Mach number and apogee altitude even in the presence of external perturbations.

Keywords: STORT, Sounding Rocket, Flight Experiment, Hypersonic, Thermal Management

Nomenclature

g	gravity acceleration	m/s^2
q	dynamic pressure	Pa
T	Temperature	K
v	velocity	m/s
α	angle of attack	-
β	yaw angle	-

Acronyms /Abbreviations

3 DOF	Three Degrees of Freedom
CFD	Computational Fluid Dynamics
C/C-SiC	Carbon Fibre Reinforced Silicon Carbide
CFRP	Carbon Fibre Reinforced Polymer
CIRA86	COSPAR International Reference Atmosphere
CMC	Ceramic Matrix Composite
CoG	Center of gravity
DAQ	Data Acquisition System
DLR	German Aerospace Center
DMARS	Digital Miniature Attitude Reference System
FADS	Flush Air Data Sensing
IMU	Inertial Measurement Unit
IO	Improved Orion
Ma	Mach number
MORABA	Mobile Rocket Base of DLR
Re	Reynolds number
RLV	Reusable Launch Vehicle
SWBLI	Shock Wave Boundary Layer Interaction
TC	Thermocouple
TPS	Thermal Protection System
USSA76	US Standard Atmosphere 1976

1. Introduction

Simulation based design of flight hardware is one of the long-term goals of the DLR's research programs. It requires high quality validation data, which is representative for the real flight environment. Since ground testing facilities have limitations to duplicate the flight environment, availability of flight data is essential. But, in case of spacecraft development this task is very challenging, since the number of flight experiment and availability of the flight data is very limited. This requires a complementary validation approach using ground and flight testing for gathering reliable data and validation of numerical tools. Numerical tools have still shortcomings in modelling high temperature gas phenomena and gas surface interaction in such environments [1,2]. This again requires material characteristics to be available for a very broad temperature range. Therefore, ground characterization and qualification of hot structures have to be carried out using modern diagnostic methods. Since ground experiments cannot duplicate the flight environment completely, performing successful flight experiments to achieve the a. m. goal is essential.

The success of SpaceX's space transportation approach triggered a worldwide uptick in reusable launcher activities. Multiple reuses of the most expensive

first stage is the focus of most concepts. Recent studies show that reusability becomes feasible if the separation of the first stage takes place at Mach numbers between 9 and 12. Simulation of this flight environment in ground facilities is limited and requires further data of flight experiments. Hypersonic flight experiments by means of multi stage sounding rocket configurations are the most cost-efficient options to gather valuable flight data. Using available two stage sounding rocket configurations consisting of S31/S30 stages the achievable Mach number for a payload mass of approx. 300 kg is mostly limited to around 6. SHEFEX-II flight experiment could reach Mach numbers up to 10 using a much stronger motor combination of S40 and S44 [3], which are not currently available. This limitation in combination with the target payload mass forced the DLR's flight experiment REFEX to focus in guidance and navigation during return flight at Mach numbers from 5 down to subsonic speeds [4]. Therefore, aerothermal loads on hot structures are beyond the REFEX project goals.

Past DLR hypersonic flight experiments reached peak mach numbers of up to 10 [3, 5, 6], but the test phase with high aerothermal loads were less than 30 seconds. The actually achieved high structure temperatures were not close to the upper limit values of hot structures and materials. To close this gap and achieve higher Mach numbers the flight experiment STORT (Key Technologies for High Speed Return Flights of Launcher Stages) uses a three-stage sounding rocket configuration. In addition, a suppressed trajectory the third stage should increase integral heat load on the structures.
The past DLR's hypersonic flight experiments reached high numbers up to 10 [5, 6, 8]. But the test phase with high aerothermal loads were less than 30 seconds. Therefore, an additional maneuver will keep the third stage of the STORT configuration within a suppressed trajectory with high integral thermal loads. The main objectives of the STORT flight experiment will be described in the next chapter.

After the explaining of main objectives of the STRORT flight experiment in the first chapter, the flight configuration with major payloads is described in the second chapter, which also includes target properties of the flight trajectory. The first data of the STORT flight experiment will be discussed in the third chapter. Concluding remarks describe the main achievement but also next steps of the post flight analysis.

2. STORT Flight Configuration and Payloads

The main scientific objective of the STORT flight experiment is gathering data on aerothermal heating and structural response during a hypersonic flight of long duration with high integral heat loads. As shown in **Figure 1** the vehicle consists of three stages: the S31 first stage, the S30 second stage, and the Improved Orion (IO) third stage. The scientific payload is mounted atop the IO motor; there is an active stage separation system between the S30 and IO motor, but no payload separation system.

Figure 1: STORT three-stage flight configuration.

As shown in **Figure 2** the forebody section of the payload section is made of CMC based high temperature structure [7]. The massive ceramic blunt nose and the four downstream segments are instrumented with pressure sensors, heat flux gauges and thermocouples. Based on the experience of previous flight experiments SHEFEX-I and SHEFEX-II, a slender forebody followed by a segment with three canards acting as thermal management experiments have been selected as main scientific payloads [2,3,5].

The ceramic panels of the forebody with a thickness between 5.2 mm and 8.6 mm were equipped with different types of sensors to measure the temperature, pressure, and heat flux distribution on the TPS. These panels are mounted to an aluminum substructure via special ceramic supports. Between the ceramic TPS and the substructure, a thick insulation is used for thermal isolation of the payload interior. Special interfaces, mainly for the pressure and heat flux sensors, have been constructed using spring loaded devices to ensure a flush mounting with the TPS panel surface [5,6,8]. To verify the design of these interfaces concerning the temperature resistance of the metallic parts several transient thermal analyses have been performed.

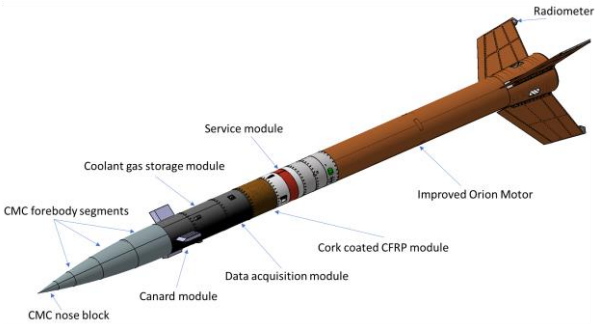

Figure 2: STORT experiments integrated into the third stage.

The ceramic panels of the forebody with a thickness between 5.2 mm and 8.6 mm were equipped with different types of sensors to measure the temperature, pressure, and heat flux distribution on the TPS. These panels are mounted to an aluminum substructure via special ceramic supports. Between the ceramic TPS and the substructure, a thick insulation is used for thermal

isolation of the payload interior. Special interfaces, mainly for the pressure and heat flux sensors, have been constructed using spring loaded devices to ensure a flush mounting with the TPS panel surface [5,6,8]. To verify the design of these interfaces concerning the temperature resistance of the metallic parts several transient thermal analyses have been performed.

The instrumentation concept of the forebody is derived from previous DLR flight experiments [9,10]. The instrumentation of CMC panels along the lines at 0° and 180° is exactly the same. This is also the case for 90° and 270° lines. For the temperature measurement of the hot structure, different types of thermocouples are used. Kulite pressure transducers of the type XTEH-7L-190 are used for the measurement of the absolute pressure. For the FADS system in the massive C/C-SiC nose, the transducers are mounted to the aluminum structure directly behind the C/C-SiC nose in order to keep the tubing length as short as possible [6,8].

Three canards, which are exposed to severe aerothermal loads during long duration hypersonic flight, have different roles for thermal management experiments. An active cooling system with monitoring instrumentation is implemented into the first fin. A passive thermal management system in the second fin should also keep the leading-edge temperature below a certain level. Due to previous activities DLR has a certain expertise on passive and active thermal management systems [11,12]. All three canards of the STORT flight configuration have the same interior structural design but different thermal management concepts. The reference canard is made of the standard C/C-SiC material. This canard doesn't have any thermal management, but is heavily instrumented to study the Shock-Wave-Boundary-Layer-Interaction (SWBLI) around the canard. The ceramic material of the second one uses highly conductive carbon fibres to enhance passive cooling by means of heat conduction inside the structure.

An active cooling system with monitoring instrumentation is implemented into the first canard. It is known that film cooling or transpiration cooling lead to the contamination of the flow. It changes flow features and makes the interpretation of the flight data difficult. Therefore, the active cooling system of STORT is based on the impingement cooling of the rear surface of the canard leading edge. Multiple injection slots should allow an almost homogenous supersonic impingement of the coolant to the rear inside surface of the C/C-SiC leading edge.

For in-situ monitoring of potential anomalies of the combustion chamber and nozzle components, a radiometer system consisting of three radiometers with different spectral ranges has been developed. It is mounted to the rear tip of fin inside a protection housing. To acquire the data of all sensors distributed in different segments of the flight configuration, a special acquisition system is needed. The sensor data of the forebody and three canards is acquired by a data acquisition system which is distributed in three units placed in the DAQ module.

STORT also included the maiden flight of an Inertial Measurement Unit (IMU) developed at MORABA. The IMU features a strapdown design and contains three fiber-optic gyroscopes (FOG) and three quarz servo-accelerometers for measuring angular velocities respectively linear accelerations about the body-fixed axes. Furthermore, the IMU features interfaces for connecting external GNSS receiver as well as an additional high-resolution mode with limited acceleration range that can be used for micro-gravity phases.

The trajectory is designed to feature a low apogee of approximately 45 km and a comparatively far impact ground range of more than 400 km. This requires the use of a low launching elevation angle as well as a coast phase following first stage burnout to allow for the gravity turn to reduce the trajectory angle. To achieve a cost-efficient flight experiment, the vehicle concept is based around an inherently safe, passively fin-stabilized sounding rocket design. To reduce the influence of wind and other factors that are difficult or impossible to correct for a priori, the third stage ignition time is determined on board based on the actual trajectory rather than the nominal trajectory. The on-board computer ignites the upper stage such that the trajectory deviation with regards to apogee and impact ground range is minimized.

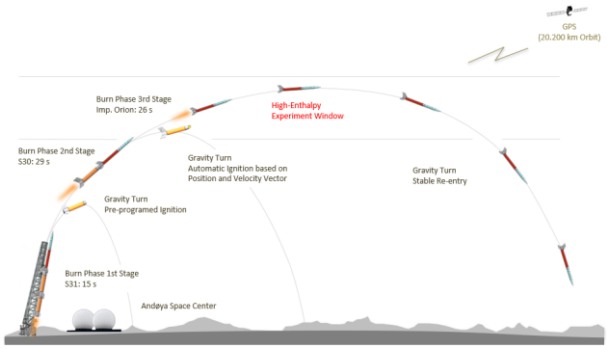

Figure 3: STORT engineering science payloads.

The first stage motor S31 is equipped with 6 fins and has a nominal burning time of 11.5 seconds. Its passive separation takes place 11.5 seconds after lift-off and leads to approx. 5 km apogee and 6.2 km impact down range. Thee second stage S30 with four stabilizing fins is ignited after a coast phase of a few seconds later and has a thrust phase of 29 seconds. Roughly nine seconds after its burn-out it is separated actively at an altitude of 24 km.

The ignition point of the third stage Improve Orion motor is extremely important for the achievement of mission goals. To ensure that the experiment conditions in terms of Mach number and apogee altitude can be reached even in the presence of perturbations, a dispersion reduction method is employed where the on-board computer chooses the optimum third stage ignition time such that the actual trajectory best matches the nominal trajectory with regards to the apogee altitude and impact ground range. To accomplish this, a reduced 3 DoF trajectory simulation is implemented on the flight computer. Predicted altitude and ground range of all three motors is shown in **Figure 4**.

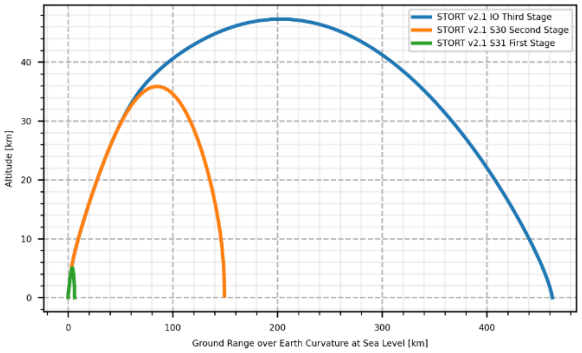

Figure 4: STORT first, second and third stage altitude over ground range.

Depending on the position and velocity vector the ignition time of the third stage is determined on-board. All these single events yield an expected flight profile in terms of Mach number shown in **Figure 5**. According to these predictions the target Mach number of 8 can be reached for a flight duration of more than 100 seconds.

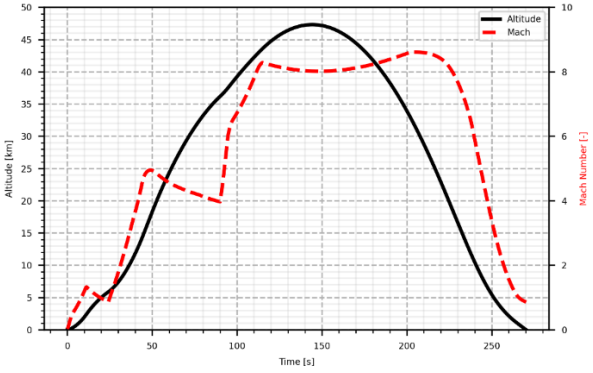

Figure 5: STORT third stage and payload altitude and Mach number (right).

Table 1 summarizes the planed main events of the STORT flight experiment.

Table 1: STORT Trajectory key events.

Event	Time [s]	Altitude [km]
S30 Motor Ignition	0	0.04
Launch Rail Exit	0.73	0.06
Spin Up Motor Ignition	0.84	0.07
Mach 1	8.39	1.45
S31 Motor Separation (passive)	11.5	2.48
S30 Motor Ignition	24	5.8
Maximum Dynamic Pressure	44.3	14.22
S30 Motor Burnout	51.1	18.7
S30 Motor Separation (active)	60.01	23.87
IO Motor Ignition	88	34.69
IO Motor Burnout	113	42.08
Apogee	141.9	45.73
Impact	265.4	0.0

3. Flight Experiment

The assembly of payload segments with a mass of approx. 200 kg and 3.5 m total length mass was carried out in a separately from the motor preparation (Figure 7: STORT payload modules.Figure 6). The main challenge was the integration of the instrumentation into the CMC nose segments and the canard module. Due to limited available space the wire harness situation created some difficulties. Operation of the high-pressure nitrogen supply for the active cooling experiment took a bit longer than planned because of gas leakage at one of the interfaces. A further time-consuming part was the verification of the communication between the service module and telemetry station. Downstream of five CMC segments the canard module with three integrated canards are placed. The outer surfaces of this module and das supply tank segment and data acquisition module were coated with a zirconia coating for thermal protection. All modules further downstream featured a cork ablator based thermal protection (Figure 7).

Figure 6: Preparation of the STORT payload modules.

Figure 7: STORT payload modules.

After completion of the assembly and verification of data communication to the data acquisition system and telemetry station, the payload was transferred to the motor launcher assembly block. Figure 8 shows the main geometrical features of the three stages configuration. The total length of the vehicle is 13.5 m. While the diameter of the first and second stages was 557 mm, the third stage (Improved Orion) and payloads have an external diameter of 356 mm. The total liftoff mass was 3009kg.

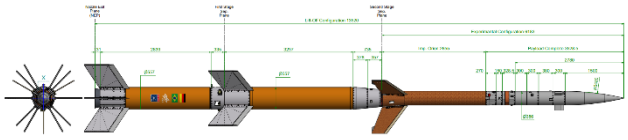

Figure 8: STORT three stage configuration.

After several verification tests in particular concerning mechanical and electrical arming and test countdowns, the STORT flight configuration was prepared for the launch at 68° elevation and 330° azimuth (Figure 9, left). In addition to the wind profile, the state of rain clouds density was one of the key decision criteria for the launch, since signature measurements using ground base infrared camera system are heavily depending on it. Finally, in the early morning of 26 June 2022, the STORT flight experiment on top of three-stage rocket configuration launched from the Andøya Space launch site in northern Norway (Figure 9, right).

Figure 9: STORT Flight experiment at the launch pad of Andoya Space Launch Site (left) and launch event (right).

As planned the first stage S31 burned out 12 seconds after lift-off and reached a velocity of 429 m/s at an altitude of 2585 m (Figure 10). Approx. 12.5 seconds after the passive separation of S31 the second stage S30 was ignited and burned around 21 seconds. At flight time point of 45.5 seconds the velocity and altitude were 1384 m/s and 14527 m, respectively. As mentioned before the ignition time point of the third stage Improved Orion was performed by using actual position and velocity vector data with a 3D flight dynamics simulation on-board. The ignition occurred 81 seconds after the lift-off at an altitude of approx. 29000 m.

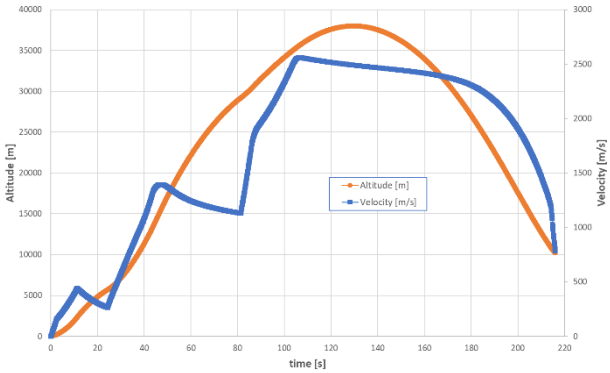

Figure 10: Altitude and velocity profiles of the STORT flight over the time.

The third stage with scientific payloads reached a flight speed of 2557 m/s, i.e. Mach number of 8.26 (USSA76 atmospheric model), at an altitude of 36 km and finally reached apogee of its trajectory at an altitude of 38 km at a velocity of 2497 m/s, which corresponds to a Mach number of 8.0 (Figure 11). It then descended into the Atlantic Ocean roughly 380 km away from the launch site. During this hot hypersonic flight phase extensive measurement data of the scientific payloads and vehicle was transmitted to the ground station.

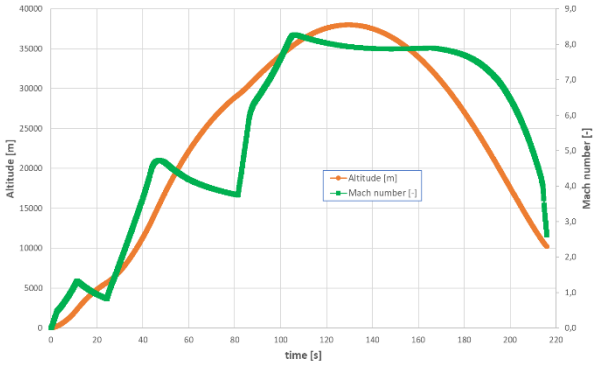

Figure 11: Altitude and Mach number profiles of the STORT flight over the time.

Figure 12 shows the Reynolds number and Mach number map of the flight using two different atmospheric models, i.e. standard US atmosphere model USSA76 and CIRA86 model. The difference between the two becomes particularly visible at high. The final selection of the atmospheric model will be carried out later after comparing these data with the data measured with balloon before the flight. At Mach 5 the unit Reynolds numbers achieved during ascent and descent are $1.95*10^6$ and $2.89*10^7$. The unit Reynolds number of 10^7 is achieved during scent at Mach number 4.4 @ altitude of 29600 m and during descent at Mach 7.2 @ altitude of 23200 m. The Reynolds number at maximum Mach number 8.26 (USSA76) is $1.3*10^6$.

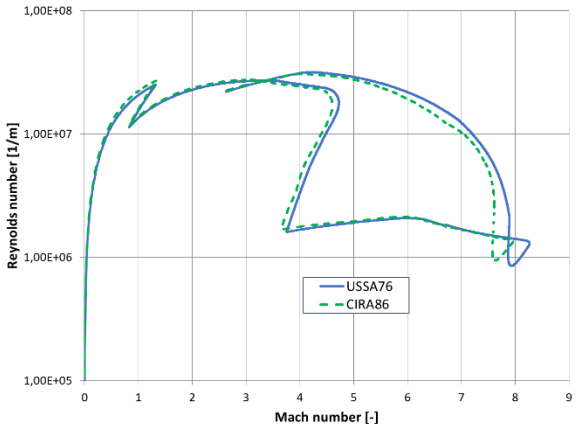

Figure 12: Altitude and Mach number profiles of the STORT flight over the time.

The 38 km apogee reached during flight is below the target value of 45.73 km (**Table 1** and Figure 10). The reason for this deviation is a calibration error during the hardware-in-the-loop tests. However, flying at Mach numbers beyond 8 at lower altitudes means higher dynamic and aerothermal loads, thus the STORT payloads were actually exposed to even more severe conditions than anticipated. The forebody of STORT is an ogive and has a total length of 1500 mm (Figure 13). As mentioned before the forebody consists of a massive nose with a radius of 2.5 mm and four downstream segments with CMC shell structures as thermal protection. The canard segment of 300 mm length includes three canards, which use again a CMC shell as thermal protection.

Figure 13: Geometry of the forebody and canard module (lift) and thermocouple positions in the nose section(right).

The CMC node block was instrumented with one type S thermocouple (TS002V) and two type K thermocouples (TS003V and TS004V) with a diameter of 1 mm and 0.5 mm, respectively. The positions of thermocouples are shown in Figure 13 (right). **Table 2** contains the exact position of sensors with reference to the coordinate system defined in Figure 13 (left).

Table 2: Positions of selected sensors along the forebody.

sensor name	x [mm]	ϕ [°]	surface distance [mm]
TS002V	34	0	5
TS003V	150	180	9
TS004V	150	0	3
TK005V	300	45	2
TK013V	550	45	2
TK021V	800	45	2
TK037V	1400	45	2
PK005V	300	0	0 (port), 38 mm (sensor)
PK007V	550	0	0 (port), 38 mm (sensor)
PK009V	800	0	0 (port), 38 mm (sensor)
PK011V	1400	0	0 (port), 38 mm (sensor)

The first CMC shell structure downstream of nose was equipped with type K thermocouples of 0.5 mm in diameter at 45° in circumferential direction below the surface. Pressure ports (PK005V, PK007V, PK009V and PK011V) were mounted at the same axial position as the thermocouples (TK005V, TK013V, TK021V TK021V) but along the different raw at 0° in circumferential direction. They were connected to Kulites sensors, which were mounted to the metallic substructure of the vehicle.

At sea level before launch all pressure sensors measure the same pressure of approx. 1000 hPa (Figure 14). A gradual pressure decrease along the axial distance from the nose is visible along the complete flight trajectory. The first small peak around 8.5 seconds is a result of sonic speed limit passage. The second peak at 24 seconds after lift-off is caused by the ignition of the second stage S30. The acceleration by means of the Improved Orion ignition around 85 seconds is also clearly visible. The pressure data during descent flight around 180 seconds after take-off indicates some fluctuations. After this time point the data becomes noisy. A significant peak followed by a data transmission interruption will be discussed with the data of other sensors later.

Figure 15 shows measured temperatures inside the CMC nose block. As mentioned before the thermocouple TS002V is a type S thermocouple and positioned in axial

direction 34 mm from the nose tip (Figure 13). It is mounted to the block 5 mm beneath the surface. Measured temperature history correlates nicely with the with motor ignition and separation times as shown in Figure 10 and Figure 11. The maximum temperature of 1382 K is reached at the flight time point of 208 seconds, which corresponds to a Mach number of 5.3 at 13.8 km altitude. The other two type K thermocouples are positioned 150 mm downstream of the nose tip (see **Table 2**) but are in different distances from the surface (Figure 13). Thermocouple TS003V closer to the surface (3 mm in contrast to 9 mm distance of TS004V) and measures higher temperature. It shows also a faster response to the potential increase of aerothermal loads at the flight time point around 190 to 200 seconds. An increase of the temperature followed by a sudden decrease at this flight time point will be discussed later.

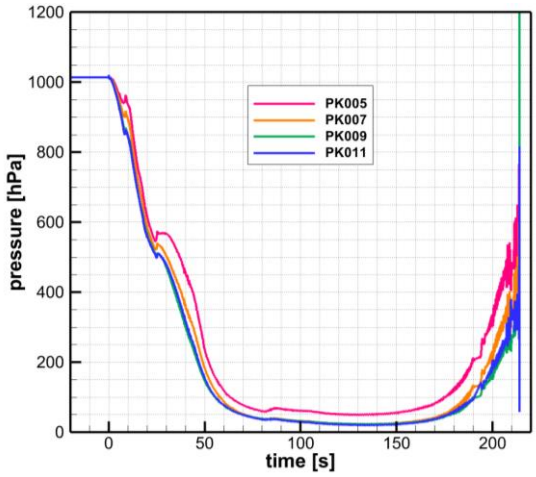

Figure 14: Measured pressure history along the forebody.

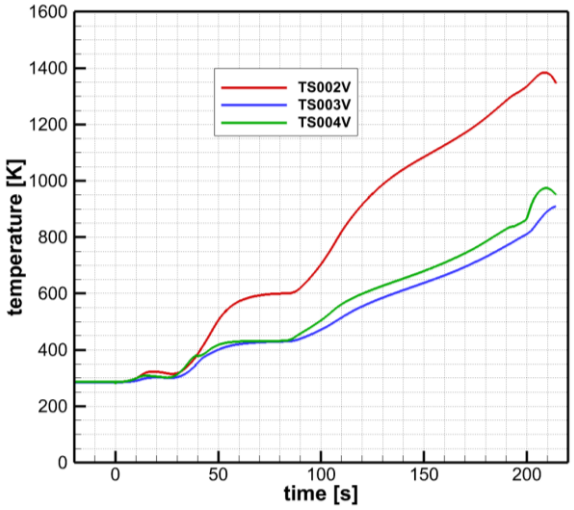

Figure 15: Measured temperatures of the CMC nose block.

The type K thermocouples TK005, TK013, TK021 und TK037 are integrated at 2 mm beneath the surface of CMC four shells along one raw as defined in Fehler! Verweisquelle konnte nicht gefunden werden.. It is well known that even slight differences in integration process can have a remarkable on the response time of thermocouples [5]. Therefore, measured gradients after the ignition of the second stage S30 do not follow expected temperature evolution along the flow axis of the forebody. But, in the flight phase at Mach numbers above 6 (after 85 seconds) the nose becomes hot and clear differences in thermocouple data are visible. TK005 is closer to the nose block and shows steeper temperature gradients compared to other sensors (Figure 16). Thermal conduction from the hot nose to the first shell segment in addition to convective heating is the main reason of this behavior.

Similar to all four thermocouples TK013 of the second CMC shell (third segment of the complete forebody) detects heat flux gradients due to the ignition and burn-out of all three stages clearly. The temperature increase at flight time points of 186 seconds and 194 seconds could be caused by other effects. This last temperature gradient visible at 182 seconds and 180 seconds for the third and fourth (last) CMC shell segments, respectively. The Mach number at 180 seconds is 7.7 at an altitude 26.6 km during descent flight. This corresponds to a Reynolds number of 4.5 10^6. This raises the question whether laminar to turbulent transition of the boundary layer flow is responsible for it.

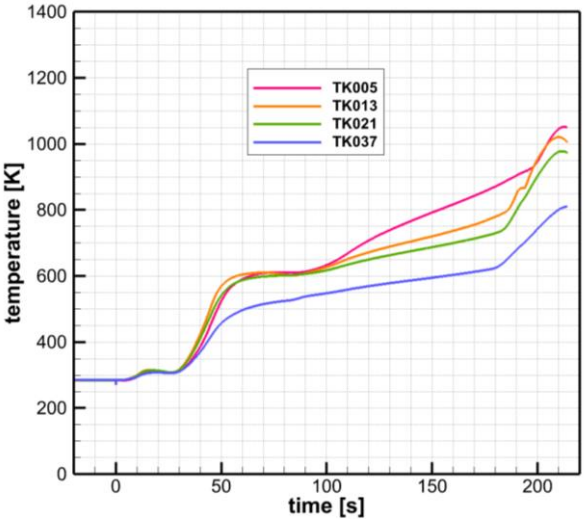

Figure 16: Measured temperatures of the CMC shell of the second segment.

But, the acceleration data of the DMARS system brings some complexity into the interpretation (Figure 17). Longitudinal acceleration data follows expected ignition, thrust and burn-out phases of all three stages perfectly. 170 seconds after lift-off the axial deceleration of the vehicle increases. At this point the Mach number is around 8 at lower altitude of 31 km. But, at the same time in both lateral and normal directions a short acceleration peak followed by an oscillatory behaviour around the zero-g line is visible. Around 210 seconds these oscillations are enhanced and lead to strong acceleration peaks in all three directions. It corresponds to the flight trajectory point with a Mach number of 4.9 at 13 km altitude. A detailed analysis of the anomaly is still under investigation. The data of the new Inertial

Measurement Unit (IMU) developed at MORABA showed a good agreement with the DMARS data.

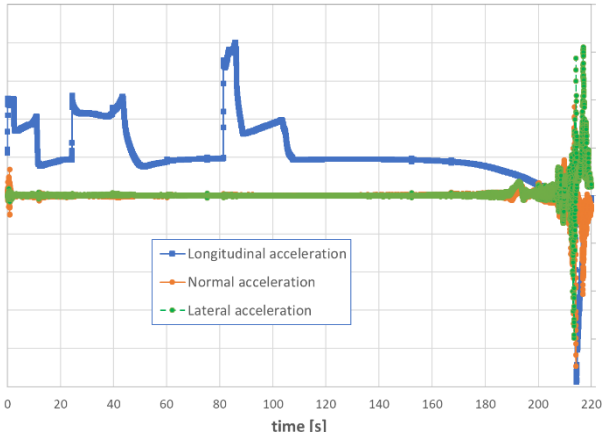

Figure 17: Measured accelerations during STORT flight.

Measured roll angular rate history shows an interesting behavior (Figure 18). An increase of the roll rate during active thrust phases is followed by a slight decrease for the timeslots without thrust is observed. The born-out time of 11.5 seconds and 44 seconds of both S31 and S30 motors correlates to the roll rate decrease points. Separation of the S30 motor in the no thrust phase around 60 seconds causes also a roll rate increase, which is followed by a decrease until the ignition of the IO motor at the time point of 80 seconds. The high thrust phase of 4 seconds leads to a further increase of the roll rate, which changes its slop during sustain phase of IO. At the burn-out point of IO motor around 113 seconds the almost maximum rate of 870 deg/seconds is reached. Until the apogee point of 132 seconds the roll rate remains around 900 deg/s and starts to decrease during descent flight due to aerodynamic damping effects.

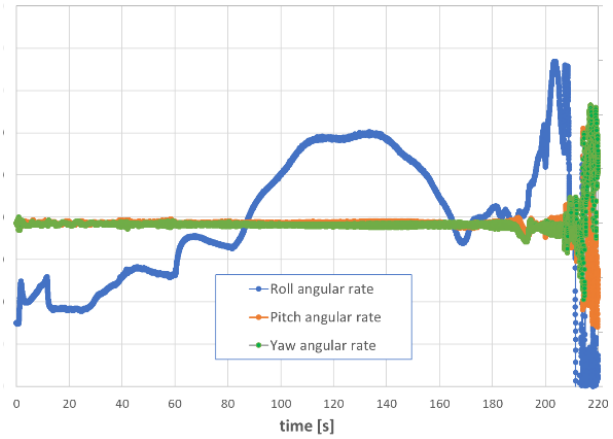

Figure 18: Measured angular rates during STORT flight.

For in-situ monitoring of potential anomalies of the combustion chamber and nozzle components a radiometer system consisting of three radiometers with different spectral ranges has been developed. It is mounted to the rear tip of fin inside a protection housing [13].

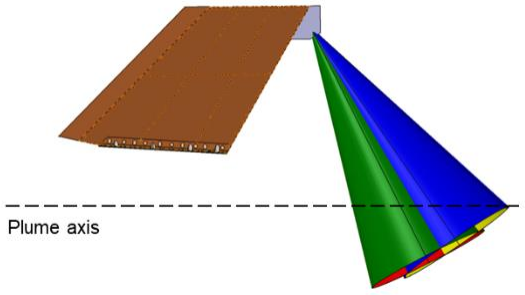

Figure 19: View field of radiometers integrated in the aft part of the fin.

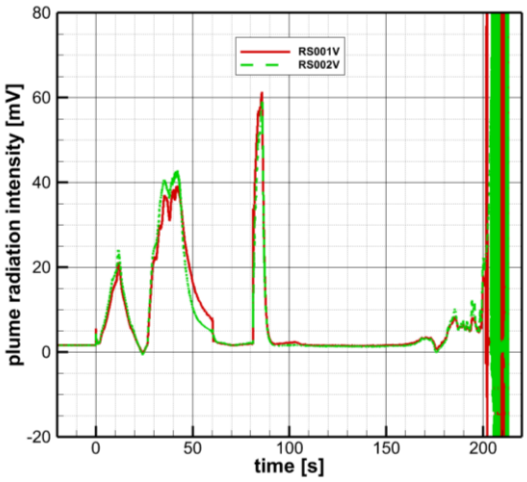

Figure 20: Plume radiation intensity measured with radiometers.

The Shock Wave Boundary Layer Experiment (SWBLI) was one of the key aerothermal experiments of the STORT flight experiment [13]. Heat flux and pressure sensors with a fast response time mounted around the canard measured the foot print of the shock wave boundary layer interaction on the canard module surface. The instrumentation design of this payload is carried out in cooperation with the University of Arizona using experimental and numerical tools. Post flight data processing of this experiment is still ongoing.

4. Concluding remarks

The long duration hypersonic experiment STORT with more than 60 seconds Mach 8 flight at an altitude between 30 km and 38 km has been carried out on top of a three-stages sounding rocket configuration successfully. The instrumentation of the main scientific payloads like the forebody, three fixed canards, thermal management experiments and shock wave boundary layer interaction experiment delivered unique data of a hypersonic flight. Three radiometers mounted to the rear part of the third stage fins measured plume radiation in different spectral ranges. A reduced in-flight 3 DoF trajectory simulation implemented on the flight computer allowed to achieve experiment conditions in terms of Mach number and apogee altitude by means of an on-board selected optimum third stage ignition time point. A

new Inertial Measurement Unit (IMU) developed at DLR has been flight qualified.

STORT flight had a hypersonic flight phase at Mach numbers between 5.0 and 8.2 with a duration of 126 seconds. The duration of a flight phase above Mach 8 at altitudes between 30 km and 38 km was more than 60 seconds. The apogee of 38 km was lower than the target value of 45.7 km, which led to higher aerothermal loads, since the Mach number range was comparable to the planned values. The detailed post flight analysis of the flight data is progress and will be completed in the coming a few months.

Acknowledgment

The research project STORT including the flight experiment was funded by the DLR's Program Directorate for Space Research and Development.

References

1. Mack, A.; Schäfer, R.; Gülhan, A.; Esser, B.; IMENS Flowfield Topology Changes due to Fluid-Structure Interaction in Hypersonic Flow Using ANSYS and TAU. in C. Breitsamer, B. Laschka, H. J. Heinemann, R. Hilbig (Eds.), New Results in Numerical and Experimental Fluid Mechanics IV, Springer, pp. 196-203, 2004.
2. Barth, T., "Aerothermodynamische Untersuchungen facetierter Raumfahrzeuge unter Wiedereintrittsbedingungen," Ph.D. Thesis, Inst. of Aerospace Thermodynamics, Univ. of Stuttgart, Stuttgart, Germany, 2010.
3. Weihs, H., Longo, J., and Gülhan, A., "Sharp Edge Flight Experiment SHEFEX," Fourth European Workshop on Thermal Protection Systems and Hot Structures Conference Proceedings, ESA SP-521, Noordwijk, The Netherlands, 2002.
4. Peter Rickmers, Waldemar Bauer, Guido Wübbels, and Sebastian Kottmeier, "Refex: Reusability flight experiment - a project overview," in 8th European Conference for Aeronautics and Space Sciences (EUCASS), 2019.
5. Ali Gülhan, Dominik Neeb, Thomas Thiele and Frank Siebe; Aerothermal Postflight Analysis of the Sharp Edge Flight Experiment-II. Journal of Spacecraft and Rockets, DOI: 10.2514/1.A33275. ISSN 0022-4650.
6. Thiele, T., Neeb, D., and Gülhan, A., "Post-Flight Hypersonic Ground Experiments and FADS Flight Data Evaluation for the SHEFEX-II Configuration," Proceedings of 8th European Symposium on Aerothermodynamics for Space Vehicles, ESA, March 2015.
7. Guiseppe D. di Martino, Thomas Reimer, Lucas Dauth, Luis Baier; Structure Design of a Sounding Rocket Forebody with a Segmented Filament Winding-Ceramic Matrix Composite Thermal Protection System, HiSST: 2nd International Conference on High-Speed Vehicle Science Technology, 11-15 September 2022, Bruges, Belgium.
8. Gülhan, Ali und Thiele, Thomas und Siebe, Frank und Kronen, Rolf und Schleutker, Thorn (2018) Aerothermal Measurements from the ExoMars Schiaparelli Capsule Entry. Journal of Spacecraft and Rockets. American Institute of Aeronautics and Astronautics (AIAA). DOI: 10.2514/1.A34228 ISSN 0022-4650.
9. T. Thiele, A. Gülhan, H. Olivier; Instrumentation and Aerothermal Postflight Analysis of the Rocket Technology Flight Experiment ROTEX-T, Journal of Spacecraft and Rockets, Vol. 55, No. 5, September–October 2018.
10. A. Gülhan, F. Klingenberg, F. Siebe, A. Kallenbach and I. Petkov; Main Achievements of the Sounding Rocket Flight Experiment ATEK, IAC, Dubai, October 25-29, 2021, IAC-21,D2,6,4,x62713.
11. B. Esser et al., "Innovative Thermal Management Concepts and Material Solutions for Future Space Vehicles", Journal of Spacecraft and Rockets, vol. 53 (6), pp. 1051-1060, 2016. doi: 10.2514/1.A33501.
12. Böhrk, H., Kuhn, M., and Weihs, H.; "Concept of the Heat Balance of the Transpiration-Cooled Heat Shield Experiment AKTIV on SHEFEX II," Proceedings of the 6th European Workshop on Thermal Protection System and Hot Structures, European Space Agency, Noordwijk, The Netherlands, April 2009.
13. A. Gülhan, S. Willems, F. Klingenberg, D. Hargarten, M. Hörshgen-Eggers; Sport Flight Experiment for High Speed Technology Demonstration, Dubai, October 25-29, 2021, IAC-21,D2,6,5,x62714.